Published in final edited form as:
J Immunol. 2012 September 15; 189(6): 3007–3017. doi:10.4049/jimmunol.1201483.

Globosides but not isoglobosides can impact the development of invariant natural killer T cells and their interaction with dendritic cells[1]

Stefan Porubsky[*,††], **Anneliese O. Speak**[†], **Mariolina Salio**[‡], **Richard Jennemann**[*], **Mahnaz Bonrouhi**[*], **Rashad Zafarulla**[§], **Yogesh Singh**[§], **Julian Dyson**[§], **Bruno Luckow**[¶], **Agnes Lehuen**[||], **Ernst Malle**[#], **Johannes Müthing**[**], **Frances M. Platt**[†], **Vincenzo Cerundolo**[‡], and **Hermann-Josef Gröne**[*]

[*]Department of Cellular and Molecular Pathology, German Cancer Research Center, Heidelberg, Germany

[†]Department of Pharmacology, University of Oxford, Oxford, UK

[‡]MRC Human Immunology Unit, Weatherall Institute of Molecular Medicine, John Radcliffe Hospital, Oxford, UK

[§]Section of Immunobiology, Department of Medicine, Imperial College London, London, UK

[¶]Klinikum der Universität München, Medizinische Klinik und Poliklinik IV, Nephrologisches Zentrum, Arbeitsgruppe Klinische Biochemie, Munich, Germany

[||]Institut National de la Santé et de la Recherche Médicale Unité 986, Hôpital Cochin/St Vincent de Paul, Paris, France

[#]Institute of Molecular Biology and Biochemistry, Center for Molecular Medicine, Medical University of Graz, Austria

[**]Institute for Hygiene, University of Münster, Germany

[††]Institute of Pathology, University Medical Center Mannheim, University of Heidelberg, Mannheim, Germany

Abstract

Recognition of endogenous lipid antigen(s) on CD1d is required for the development of invariant natural killer T (iNKT) cells. Isoglobotrihexosylceramide (iGb3) has been implicated as this endogenous selecting ligand and recently suggested to control over-stimulation and deletion of iNKT cells in α-galactosidase A-deficient mice ($\alpha GalA^{-/-}$, human Fabry disease), which accumulate isoglobosides and globosides. However, the presence and function of iGb3 in murine thymus remained controversial. In this paper we generate a globotrihexosylceramide (Gb3) synthase deficient mouse ($Gb3S^{-/-}$) and show that in $\alpha GalA^{-/-}/Gb3S^{-/-}$ double knockout mice, which store isoglobosides but no globosides, minute amounts of iGb3 can be detected by high performance liquid chromatography. Furthermore we demonstrate that iGb3-deficiency does not only fail to impact selection of iNKT cells, in terms of frequency and absolute numbers, but also does not alter the distribution of the T cell receptor (TCR) complementarity determining region 3

[1]**Grant support:** This work was supported by grants from the Deutsche Forschungsgemeinschaft to H.-J. Gröne and S. Porubský (SFB 938). A. O. Speak was supported by the Medical Research Council, UK (G0700851). V. Cerundolo and M. Salio were supported by Cancer Research UK (C399/A2291), the UK Medical Research Council and The Wellcome Trust (084923/Z/08/Z).

Corresponding authors: Hermann-Josef Gröne and Stefan Porubsky, Department of Cellular and Molecular Pathology, German Cancer Research Center, Im Neuenheimer Feld 280, 69120 Heidelberg, Germany; h.-j.groene@dkfz.de and s.porubsky@dkfz.de; Telephone: +49 6221 424350; Fax: +49 6221 424352.

Europe PMC Funders Author Manuscripts

of iNKT cells. Analyzing multiple gene targeted mouse strains, we demonstrate that globoside, rather than iGb3, storage is the major cause for reduced iNKT cell frequencies and defective antigen presentation in $\alpha GalA^{-/-}$ mice. Finally, we show that correction of globoside storage in $\alpha GalA^{-/-}$ mice by crossing them with $Gb3S^{-/-}$ normalizes iNKT cell frequencies and dendritic cell (DC) function. We conclude that, although detectable in murine thymus in $\alpha GalA^{-/-}/Gb3S^{-/-}$ mice, iGb3 does not influence either the development of iNKT cells or their interaction with peripheral DCs. Moreover in $\alpha GalA^{-/-}$ mice it is the Gb3-storage that is responsible for the decreased iNKT cell numbers and impeded antigen presentation on DCs.

INTRODUCTION

Natural killer T (NKT) cells represent a discrete T cell population expressing T cell receptor (TCR) αβ together with NK cell surface markers such as NK1.1 (CD161) (1). A subset of NKT cells expresses an invariant TCR α-chain (Vα14-Jα18 in mouse and Vα24-Jα18 in human) with a restricted set of TCR β-chains (Vβ2, Vβ7, Vβ8.2 in mouse and Vβ11 in human) and is thus referred to as invariant NKT (iNKT or type I NKT) cells (2-5). Although constituting less than 1% of mouse lymphocytes, iNKT cells have repeatedly been shown to play an important role in tumor surveillance, in establishing peripheral tolerance, and also in defense against infections (6-10).

Unlike MHC class I and II restricted T cells, iNKT cells recognize exogenous and endogenous lipid antigens presented by non-polymorphic MHC class I-like CD1 molecules (11, 12). Several exogenous microbial lipid and glycolipid antigens recognized by iNKT cells have been identified (13, 14). The prototypical iNKT cell agonist is α-galactosylceramide (αGalCer, also referred to as KRN7000), a glycosphingolipid (GSL), which is derived from the marine sponge *Agelas mauritanius* (15, 16). αGalCer represents a specific and strong ligand for iNKT cells eliciting a rapid release of Th1 and Th2 type cytokines in large amounts.

While conventional T cells require presentation of peptide antigens on MHC class I or II molecules of cortical epithelial cells, positive selection of iNKT cells requires the presentation of an endogenous lipid antigen by CD1-molecules of double positive ($CD4^+$/$CD8^+$) cortical thymocytes (17). CD1d deletion or aberrant trafficking due to a mutation in its cytoplasmic tail interferes with the positive thymic selection of iNKT cells with the consequence of diminished iNKT cell numbers (18, 19). Nevertheless CD1 molecules alone are not sufficient for the positive selection of iNKT cells, as sphingolipid activator proteins and lysosomal proteases are also indispensable for normal iNKT cell selection (20, 21) suggesting that a lipid self antigen(s) is loaded onto CD1 in order to enable positive selection of iNKT cells (12, 22). Based on amino acid sequence, the five members of the human CD1 family have been assigned to either group I, which comprises CD1a, -b, -c, and -e molecules, or group II, which consists of the CD1d molecule. Unlike humans, mice lack group I CD1 molecules and have two group II *Cd1* genes termed *Cd1d1* and *Cd1d2*, from which only *Cd1d1* seems to encode for a functional protein (23). A variety of endogenous lipids have been demonstrated to be captured by CD1d on the secretory pathway or during endosomal-lysosomal recycling (22); the majority of them being phospholipids (including diacyl- and lyso-species, cardiolipins and plasmalogens) or sphingolipids (sphingomyelin and glycosphingolipids) (24-27). However, most iNKT cells do not respond to these lipids and the reactivity towards them is restricted to singular iNKT cell clones (28).

Based on the observation that cells deficient in glucosylceramide (GlcCer) based GSL (Fig. 1) are unable to stimulate iNKT cell hybridomas, it was suggested that the endogenous selecting ligand might be a GSL (29). Reduced iNKT cell numbers in mice deficient in the

Europe PMC Funders Author Manuscripts

β-subunit of β-hexosaminidase (*Hexb*$^{-/-}$, Sandhoff storage disease, Fig. 1) together with the well documented *in vitro* stimulatory capacity of isoglobotrihexosylceramide (iGb3) towards iNKT cells led to the conclusion that iGb3 is the endogenous lipid ligand responsible for the positive selection of iNKT cells (30, 31). However, previously we demonstrated that iGb3-synthase deficient mice (i*Gb3S*$^{-/-}$) have normal iNKT cell numbers and do not show a functional phenotype (32) suggesting that iGb3 is unlikely to be the only endogenous iNKT cell lipid ligand. Also the presence of isoglobosides and iGb3 in murine thymus remains highly controversial: mass spectrometry showed the presence of iGb3 in murine thymus (33), whereas a highly sensitive HPLC failed to detect the iGb3 in the murine thymus, a possible reason for this being that the major globotrihexosylceramide (Gb3) peak masked the putatively very low levels of iGb3 (34). Recently, it has been demonstrated that peroxisomal ether-bonded mono-alkyl glycerophosphates are potent activators of iNKT cells and that mice with absence of glyceronephosphate O-acyltransferase (GNPAT), the enzyme generating these lipids, show an altered thymic iNKT cell development (35).

Recognition of endogenous lipid antigens is also important for the function of peripheral iNKT cells which are, however, capable of indirect activation without the need for recognition of CD1d-presented microbial lipid antigens (36). According to this concept, iNKT cell activation is mediated by up-regulation and presentation of endogenous lipid antigens on CD1d upon recognition of microbial danger signals by antigen presenting cells (APCs), in concert with cytokines such as IL-12 (37, 38). Even in this setting the identity of the endogenous lipid(s) has not been fully elucidated. iGb3 was originally implicated in iNKT cell activation by TLR-ligand-activated DCs (39) and it has been argued that in α-galactosidase A deficient mice (*αGalA*$^{-/-}$, Fabry lysosomal storage disease, Fig. 1) iGb3 accumulation is responsible for overstimulation and decreased numbers of peripheral iNKT cells (40). However, more recently, GlcCer has been proposed as a relevant endogenous lipid antigen mediating iNKT cell activation in response to microbial danger signals (41).

In the present study, we have generated Gb3 synthase-deficient (*Gb3S*$^{-/-}$) mice and used them in combination with *αGalA*$^{-/-}$ storage mice, which enabled the accumulation of isoglobosides without globosides (Fig. 1). This allowed us to detect minute amounts of iGb3 in murine thymi of *αGalA*$^{-/-}$/*Gb3S*$^{-/-}$ mice. In view of this finding, we re-analyzed in detail the TCR repertoire of iNKT cells developing (in normal frequencies) in *iGb3S*$^{-/-}$ mice and demonstrated that they express a typical iNKT TCR repertoire. Moreover, comparison of *αGalA*$^{-/-}$/*Gb3S*$^{-/-}$ and *αGalA*$^{-/-}$/*iGb3S*$^{-/-}$ mice showed that it is not the accumulation of iGb3 but rather the storage of globosides that is responsible for the decreased iNKT cells numbers and altered antigen presentation on DCs in *αGalA*$^{-/-}$ storage mice. This study shows, therefore, that despite its presence in thymus, iGb3 does not mediate the positive selection of iNKT cells, and neither is it the endogenous ligand responsible for the interaction between DCs and iNKT cells in the periphery.

MATHERIALS AND METHODS

Generation of Gb3 synthase-deficient (Gb3S$^{-/-}$) mice

Clone MPMGc121J18724Q5 from the 129/Ola mouse genomic cosmid library number 121 from the German Resource Center for Genome Research (Berlin, Germany) containing the *Gb3S* (A4galt, EC 2.4.1.228) locus was used to construct a targeting vector by Red/ET homologous recombination technology (Gene Bridges, Dresden, Germany) (42). First a 9.9kb fragment corresponding to the region from 83.054.060 to 83.063.963 on chromosome 15 (NCBI m37 assembly) and bearing the *Gb3S*-gene was subcloned into the plasmid vector pBluescript M13(+) (Stratagene, Heidelberg, Germany). The coding sequence of exon 3 was then replaced by a loxP-flanked neomycin selection cassette (loxP-PGK-gb2-neo-loxP cassette, Gene Bridges, Dresden, Germany). The deleted Gb3S sequences extended from

position 83.057.694 to 83.059.066 (Fig. 2A). The targeting vector was electroporated into E14 embryonic stem cells and 384 G418-resistant clones were picked, expanded and characterized by Southern blot analysis using the 3′ and 5′ external probes (Fig. 2B), which had been generated by PCR using the following primers: 5′-CAG GCT GAA TGA CCT AAG GC-3′; 5′-GCT GCT TGT CTT CTG CGA C-3′ and 5′-GAA CTC ACC CCA TCC AAG C-3′; 5′-TGG TCA TAG TGC TGC TCT AAG C-3′, respectively. Two positive ES cell clones were detected and microinjected into C57BL/6 blastocysts. For Cre-mediated deletion of the loxP-flanked neomycin selection cassette, *Gb3S*-deficient mice were crossed with a Cre deleter strain (43). Deletion of the selection cassette was proven by PCR using the primers F2 5′-GCT TCT GAC TGC CCT TTC AC-3′ and R2 5′-TCC TTC TCC CTC AGC ATT TC-3′ (2048bp before and 498bp after deletion, Fig 2C). Mice were backcrossed for 10 generations to C57BL/6 (Charles River Wiga, Sulzfeld, Germany) prior to analysis.

Other genetically modified mice

Mice deficient for *iGb3S* (A3galt2$^{tm1.1Hjg}$, EC 2.4.1.87) were generated by our group and backcrossed for more than 10 generations to the C57BL/6 genetic background (32). Mice deficient for GalNAc-transferase (B4galnt1, EC 2.4.1.92, (44)), GM3-synthase (St3gal5, EC 2.4.99.9 (45)) and GD3-synthase (St8sia1, EC 2.4.99.8 (46)) were provided by Richard Proia; mice deficient for α-galactosidase A (αGalA, EC 3.2.1.22) by Ashok Kulkarni (47); TCRVα14-Jα281 transgenic mice by Agnes Lehuen (48). Cd1d1-deficient mice (49) were purchased from The Jackson Laboratory (Bar Harbor, Maine, USA). MyD88-deficient mice (50) were from Oriental BioService, Inc. (Kyoto, Japan). All strains were housed under specific pathogen free conditions. All animal experiments were performed in compliance with the German guidelines on animal protection and were approved by the local authority.

Organ preparation and flow cytometry

Single cell preparations from organs were prepared as described previously (32). αGalCer-loaded PE-labeled CD1d tetramers were purchased from Proimmune (Oxford, UK). PBS57-loaded PE-labeled CD1d tetramers were kindly provided by NIH Tetramer Core Facility at Emory University (Atlanta, Georgia, USA). Flow cytometry was performed as described previously (32) using the following monoclonal antibodies: anti-CD1d (clone 1B1, BD, Heidelberg, Germany); anti-CD3ε (145-2C11), anti-CD11c (HL3), anti-CD19 (MB19-1), anti-CD44 (IM7) and anti-MHCII (M5/144.15.2) (all from eBioscience, San Diego, CA, USA); anti-Gb3 (CD77, 38-13) in combination with anti-rat IgM (both from GenTex Inc., Irvine, CA, USA). Analysis of flow cytometry data was performed using Cell Quest Pro software (BD) by gating on lymphocytes in the forward and side scatter.

In vitro experiments with DCs and iNKT cells

DCs were isolated from spleens by anti-CD11c micro beads (Miltenyi Biotec, Bergisch Gladbach, Germany) and plated at 50,000/well in 100μl medium (RPMI1640 with 10% FCS, 1% penicillin/streptomycin, 1% glutamine, 1% non-essential amino acids, 1% sodium pyruvate and 1% HEPES) in 96-well plates (Greiner Bio-One, Frickenhausen, Germany). αGalCer (Avanti Polar Lipids, Alabaster, Alabama, USA) was applied overnight followed by thorough washing. Heat-killed *E. coli* were prepared from overnight cultures by exposure to 70°C for 2h and applied overnight on DCs at a bacteria:DC ratio of 10:1 followed by thorough washing. iNKT cells were enriched from livers of TCRVα14-Jα281 transgenic mice using anti-CD5 micro beads (Miltenyi Biotec) and applied at 50,000/well in 100μl medium as above. IFNγ was measured by cytometric bead array technique (BD) after co-incubating DCs and iNKT cells for 24h in case of αGalCer presentation or 5d in case that the interaction with DCs stimulated with heat-killed bacteria was assessed. Ovalbumin presentation towards MHC I and II restricted T-cell hybridomas was tested as previously described (51). For cellular cholesterol/cholesteryl ester loading experiments bone marrow-

derived DCs (BMDCs) were prepared as described (51). Cells were incubated with 50 μg/ml acetylated low-density lipoprotein (AcLDL) overnight followed by thorough washing. AcLDL was prepared following treatment of native LDL isolated as described (52) by multiple 2-μl aliquots of acetic anhydride (53).

Spectratyping

Thymic iNKT cells were enriched using 2μl PBS57-loaded PE-labeled CD1d-tetramers (NIH Tetramer Core Facility at Emory University) in a total volume of 200μl PBS with 1% BSA and 2mM EDTA at room temperature for 30 min. After washing, the cell pellet was incubated with 10μl anti-PE micro beads (Miltenyi Biotec) at 4°C for 15 min. Enrichment was performed according to manufacturer's instruction using MS-columns (Miltenyi Biotec). RNA was isolated using the acid phenol/chloroform extraction method (54). Contaminating genomic DNA was removed by digestion with RNase-free DNaseI (turbo DNA free, Ambion, Huntingdon, UK). The total amount of RNA was subjected to reverse-transcription in 20μl volume using SuperscriptII (Invitrogen, Karlsruhe, Germany) according to the manufacturer's instructions. For TCR sequencing, Vα14 and Vβ8.2 rearrangements were amplified using Vα14/Cα (5′-TCC TGG TTG ACC AAA AAG AC-3′ and 5′-CTT TCA GCA GGA GGA TTC G-3′) and Vβ8.2/Cβ (5′-GGT GAC ATT GAG CTG TAA T-3′ and 5′-AGA AGC CCC TGG CCA AGC ACA-3′) primers respectively. PCR products were cloned using the TA Cloning kit (Invitrogen Life Technologies) and sequenced using the M13R primer. Spectratyping was performed as described using Vβ2, 7 and 8.2 primers in combination with Cβ or Jβ primers (55).

HPLC

Glycolipid extraction, purification, ceramide glycanase digestion and fluorescent derivatization were performed as previously described (34). Normal phase HPLC was as previously described (34) with the exception that fluorescent detection was performed with a Waters 2475 detector (Waters, Milford, Massachusetts, USA). Oligosaccharide standards for calibration were purchased from Dextra labs (Reading, UK). Green coffee bean α-galactosidase (α1-3, 4 and 6) was purchased from Glyko Prozyme (Hayward, California, USA) and 50mU was used per digest for 48h with samples prepared for HPLC as previously described (34).

Isolation of neutral GSL

Freshly harvested spleens and kidneys were frozen in liquid nitrogen and lyophilized. Tissues were powdered and dry weight was determined. GSL were extracted with 2ml $CHCl_3/CH_3OH/H_2O$ 10:10:10 v/v/v under sonication in a water bath at 50°C for 15 min. After centrifugation at 4000rpm for 10 min, supernatants were collected and the pellets extracted again first with 2ml $CHCl_3/CH_3OH/H_2O$ (10:10:10, v/v/v) and then with $CHCl_3/CH_3OH/H_2O$ (30:60:8, v/v/v). Supernatants were combined and dried under a stream of air. Crude extracts were treated with 1ml 0.1M KOH in CH_3OH at 50°C for 4h in order to eliminate phospholipids and triglycerides. After neutralization with acetic acid and evaporation of CH_3OH, potassium acetate was removed from lipids via reversed phase column chromatography (RP18): small glass pipettes were filled with 200μl of silicagel RP18 material (Waters, Milford, MA, USA) preconditioned with 2ml each of CH_3OH, H_2O, and 0.1M potassium acetate in H_2O. Lipid extracts were suspended in 1ml of H_2O and applied to the columns. After washing with 4ml H_2O, lipids were eluted with 4ml of methanol and dried. For the separation of GSL into neutral and acidic (sialic acid-containing) components by ion exchange chromatography, glass pipettes were filled with 200μl DEAE Sephadex A25 (GE Healthcare, Uppsala, Sweden). Columns were preconditioned with 2ml CH_3OH. The lipid extracts were solved in 2ml CH_3OH and applied to the columns. Flowthroughs containing neutral GSL were collected. Neutral GSL were

eluted from the columns with additional 4ml of CH_3OH and acidic GSL with 2ml of 0.5M potassium acetate in CH_3OH. Neutral GSL were thoroughly dried and kept for several hours in a vacuum desiccator. GSL were solved in 200μl dichloroethane (DCE) and acetylated by the addition of 50μl acetic anhydride and 50μl 0.1% dimethylaminopyridine in DCE at 37°C for 1h. The reaction solvents were evaporated under a N_2 stream by the addition of 200μl toluene, three times. Glass pipettes were filled with 400μl Florisil (Merck, Darmstadt, Germany) and washed with 4ml DCE/n-hexane (4:1, v/v). The acetylated neutral GSL were solved in the same solvent mixture and applied to the columns followed by washing steps with DCE/n-hexane (4:1, v/v) and DCE, 4ml each. GSL were eluted from columns with 4ml DCE/acetone (1:1, v/v) and dried. In order to remove acetyl groups from sugar moieties, neutral GSL were solved in 0.1M KOH in CH_3OH and incubated at 37°C for 2h. After neutralization with acetic acid, the purified neutral GSL were dried and desalted by RP18 column chromatography as described above.

Thin layer chromatography (TLC)

Neutral GSL were isolated from kidneys and spleens. An amount corresponding to 2mg dry organ weight was loaded twice on two halves of a TLC plate (Merck, Darmstadt, Germany). Running solvent was $CHCl_3/CH_3OH/H_2O$ (62.5:30:6, v/v/v). The TLC plate was divided into two halves and one part was sprayed with 0.2% orcinol in 10% sulfuric acid at 120°C for 10 min to visualize the GSL. The second part was used for anti-Gb3 immunostaining. For this purpose the silicagel layer was fixed by dipping into a solution of 5% polyisobutylmethacrylate in $CHCl_3$ diluted 1:10 with n-hexane for 2 min. The plate was then dried for 10 min and unspecific binding was blocked with 1% BSA in PBS for 1h at room temperature. Polyclonal chicken anti-Gb3 antibody JM06/298-1 (56) was diluted 1:1000 in 1% BSA in PBS and the plate was incubated overnight at 4°C. After intense washing with 0.05% Tween20 in PBS, alkaline phosphatase-conjugated polyclonal donkey anti-IgY secondary antibody (Jackson ImmunoResearch Europe, Suffolk, UK) diluted 1:200 in 1% BSA in PBS was applied for 3h at room temperature. Gb3 was visualized after a repeated washing step with BCIP (Sigma, Munich, Germany) for 5 min at room temperature.

Electron microscopy

Organs were fixed in Karnovsky's glutaraldehyde (2% paraformaldehyde, 2.5% glutaraldehyde, 0.2M cacodylate buffer pH 7.4) and embedded in araldite (Serva, Heidelberg, Germany). Ultrathin sections were stained with lead citrate and uranyl acetate. Photographs were taken on an electron microscope (Zeiss EM 910, Carl Zeiss Inc. Germany).

Statistical analysis

Unpaired two-tailed Student's t-test was performed to compare data sets. Differences were considered significant if $p<0.05$. Numbers of independent observations per group are indicated for each result.

RESULTS

iGb3 is present in extremely low amounts in the murine thymus

Using a highly sensitive HPLC method we previously investigated the presence of isoglobosides, in particular iGb3, in various murine tissues (34). Despite the high sensitivity of this method, the only murine tissue with detectable iGb3 levels was the dorsal root ganglion. iGb3 was not detected in the thymus in either wild type (WT) or $\alpha GalA^{-/-}$ mice (murine model of Fabry lysosomal storage disease), in which accumulation of isoglobosides

- together with globosides - was expected (Fig. 1). However, the iGb3-peak might have remained undetected due to overlap with the more abundant Gb3 peak.

Therefore, to circumvent this obstacle, we have now generated Gb3 synthase-deficient (*Gb3S*$^{-/-}$) mice (Fig. 2). Thin layer chromatography (TLC) of kidney extracts, which are rich in globosides in WT mice, showed absence of Gb3 and its derivatives such as Gb4 in *Gb3S*$^{-/-}$ mice thereby demonstrating the successful targeted inactivation of the *Gb3S* gene (Fig. 2D).

Using the HPLC method reported previously (34), no iGb3 could be detected in the thymus of *Gb3S*$^{-/-}$ mice despite the absence of Gb3 (Fig. 3A), however, there was still a peak that co-migrated with Gb3 and had a neutral charge in the *Gb3S*$^{-/-}$ and is as yet unidentified. In order to increase the amounts of iGb3 present in tissues yet without Gb3 accumulation, *αGalA*$^{-/-}$ mice were crossed with *Gb3S*$^{-/-}$ mice to promote the storage of iGb3 if present. By this approach a minute peak at the level of the iGb3 standard could be detected in *αGalA*$^{-/-}$/*Gb3S*$^{-/-}$ mice (Fig. 3B). Consistent with it being iGb3, this peak was also susceptible to α-galactosidase digestion (Fig. 3C) and was absent in triple *αGalA*$^{-/-}$ / *Gb3S*$^{-/-}$/*iGb3S*$^{-/-}$ knockout mice (Fig. 3D). Taking into account the number of thymocytes processed for this analysis, this peak detected in *αGalA*$^{-/-}$/*Gb3S*$^{-/-}$ mice corresponded to 1619±380 molecules of iGb3 per thymocyte (mean±SEM, n=3) in this genetically manipulated cross.

iGb3S$^{-/-}$ mice express a typical iNKT TCR repertoire

Previously, we have shown that *iGb3S*$^{-/-}$ mice backcrossed for four generations to the C57BL/6 genetic background had normal iNKT cell frequencies (32). These results could now be verified after further backcrossing of the *iGb3S*$^{-/-}$ mice for more than 10 generations to the C57BL/6 genetic background (data not shown). Given the normal numbers of iNKT cells in iGb3-deficient mice, we hypothesized that the absence of iGb3 during the process of positive selection might still be reflected by a change in the CDR3 regions of their TCR α- and β-chains. In order to test this hypothesis, mRNA was isolated from enriched thymic iNKT cells of *iGb3S*$^{-/-}$ and control (*iGb3S*$^{+/-}$) mice. Vα14 chains were amplified by PCR using Vα14 and Cα constant regions primers. The canonical iNKT Vα14-Jα18 CDR3 sequence was dominant in both *iGb3S*$^{-/-}$ (22/23 sequences) and control mice (17/18) sequences (Fig. 4A). In each case, only one variant was seen which differed by a single amino acid at the same position. In the case of *iGb3S*$^{-/-}$, the variant has been previously reported in the iNKT repertoire of WT C57BL/6 mice (4). Murine iNKT cells use Vβ2, 7 and 8.2 in combination with the canonical Vα14-Jα18 alpha chain. These TCR β-chains were amplified by PCR using Vβ specific primers in combination with Cβ or, to analyze smaller components of the repertoire, with Jβ specific primers. Spectratyping of the PCR products showed highly similar CDR3 length distributions for *iGb3S*$^{-/-}$ and control iNKT cells (Fig. 4B and data not shown). Finally, sequencing of Vβ8.2 CDR3 regions showed similar Jβ segment use (Fig. 4C) and CDR3 diversity (data not shown) within *iGb3S*$^{-/-}$ and control iNKT cells. Overall, these data are consistent with iGb3 presence or absence having minimal impact on the iNKT TCR repertoire although a minor role for iGb3 in shaping TCR β CDR3 composition cannot be excluded.

Absence of globosides and subgroups of gangliosides did not influence iNKT cell numbers

In view of the fact that Gb3, in contrary to iGb3, is abundantly present in human, mouse and rat tissues and was also found in lipid eluates from soluble murine CD1d (25), we tested whether the absence of Gb3 would impact iNKT cell development. However, depletion of globosides either alone or in combination with isoglobosides did not alter the frequency of

iNKT cells in thymus, spleen or liver (Fig. S1A). Similarly, depletion of subgroups of gangliosides in mice deficient in GM3-synthase (*GM3S*), GD3-synthase (*GD3S*) and GalNAc-transferase (*GalNAcT*) had no effect on the iNKT cell population (Fig. S1B).

Absence of globosides but not of isoglobosides was able to revert the iNKT cell phenotype of αGalA$^{-/-}$ storage mice

It has been suggested by Darmoise et al. that the lowered numbers of iNKT cells in $\alpha GalA^{-/-}$ mice may be due to the accumulating iGb3 which, by overstimulation of iNKT cells, would lead to their apoptosis (40). We tested this hypothesis directly by crossing the $\alpha GalA^{-/-}$ storage mice with $iGb3S^{-/-}$ mice. In case that the accumulation of iGb3 would be indeed responsible for the lowered iNKT cell numbers in $\alpha GalA^{-/-}$ mice, then iNKT cell numbers would be expected to return to WT levels in the $\alpha GalA^{-/-}/iGb3S^{-/-}$ double knockout mice.

In line with previous reports, $\alpha GalA^{-/-}$ mice showed a significant reduction of the iNKT cell populations both in spleen and liver in comparison with WT mice (Fig. 5A). In thymus, this reduction reached statistical significance in terms of absolute iNKT cell numbers. However, in $\alpha GalA^{-/-}/iGb3S^{-/-}$ mice iNKT cell numbers were reduced to the same extent as in $\alpha GalA^{-/-}$ mice (Fig. 5A). In contrast, normalization of the iNKT cell numbers to levels indistinguishable from those in WT mice could be achieved by depletion of globosides in $\alpha GalA^{-/-}/Gb3S^{-/-}$ mice (Fig. 5A). The expression of CD1d on double positive (CD4$^+$/CD8$^+$) thymocytes or splenic DCs (CD11c$^+$/MHCII$^+$) did not differ from WT in any of these genotypes (Fig. 5B).

The normalization of iNKT cell number in $\alpha GalA^{-/-}/Gb3S^{-/-}$ but not in $\alpha GalA^{-/-}/iGb3S^{-/-}$ mice suggested that the storage of globosides, rather than the accumulation of iGb3, is responsible for the reduction of iNKT cells in $\alpha GalA^{-/-}$ mice. To prove this, we performed further biochemical analyses of spleen tissue from these mice. In parallel we also analyzed kidneys, in which globosides and galabiosylceramide (Gal_2Cer, another *Gb3S*-dependent GSL, Fig. 1) is present. As expected, accumulation of Gb3 and Gal_2Cer was detected in spleens and kidneys of $\alpha GalA^{-/-}$ mice (Fig. 6A and B). Deletion of *iGb3S* did not alter either the amount or composition of GSL stored in $\alpha GalA^{-/-}/iGb3S^{-/-}$ mice. In contrast, in $\alpha GalA^{-/-}/Gb3S^{-/-}$ mice deletion of *Gb3S* abolished the accumulation of GSL (Fig. 6A and B). Comparison of the GSL patterns between $\alpha GalA^{-/-}/Gb3S^{-/-}$ and $Gb3S^{-/-}$ mice demonstrated that no GSL other than those dependent on *Gb3S* accumulated in $\alpha GalA^{-/-}/Gb3S^{-/-}$ (and $\alpha GalA^{-/-}$) spleens and kidneys, as detected by TLC (Fig. 6A and B).

Electron microscopy further revealed that in $\alpha GalA^{-/-}$ splenocytes accumulation of GSL led to a severe disturbance of lysosomal morphology with numerous enlarged lysosomes filled with lamellar inclusions (Fig. 6C). In line with the TLC findings (Fig. 6A and B) this alteration was found also in $\alpha GalA^{-/-}/iGb3S^{-/-}$ but not in $\alpha GalA^{-/-}/Gb3S^{-/-}$ splenocytes (Fig. 6C).

In αGalA$^{-/-}$ splenocytes GSL storage led to severe impairment of antigen presentation independently of the presence of isoglobosides

Based on the severe structural derangement in $\alpha GalA^{-/-}$ splenocytes (Fig. 6C), we speculated that an impairment of antigen presentation caused by lysosomal storage could be the reason for decreased iNKT cell numbers in spleens and livers of these mice. To this end we have tested the antigen presenting capacity of DCs enriched from spleens. DCs from $\alpha GalA^{-/-}$ and $\alpha GalA^{-/-}/iGb3S^{-/-}$ were also affected by the storage of Gb3, as shown by flow cytometry with anti Gb3 antibodies (Fig. 7A). The ability of DCs from $\alpha GalA^{-/-}$ and $\alpha GalA^{-/-}/iGb3S^{-/-}$ mice to present the exogenous iNKT cell antigen αGalCer was

significantly reduced in comparison with WT mice (Fig. 7B). However, counteracting the storage by depletion of globosides restored the antigen presenting capacity of *αGalA*$^{-/-}$/*Gb3S*$^{-/-}$ DCs (Fig. 7B). iNKT cell activation by DCs that had been pre-exposed to heat-killed *E. coli* was also substantially diminished in DCs with a storage phenotype, independently of the presence of iGb3S, i.e. in *αGalA*$^{-/-}$ and *αGalA*$^{-/-}$/*iGb3S*$^{-/-}$ DCs (Fig. 7C). Reversal of storage by depletion of globosides restored microbial activation of iNKT cells to WT levels. Despite the fact that iGb3 has been postulated to mediate iNKT cell activation by DCs upon infection (39), we did not detect any decrease of this interaction when co-incubating iNKT cells and *iGb3S*$^{-/-}$ DCs pre-exposed to heat-killed *E. coli* (Fig. 7C). Furthermore, processing and (cross)presentation of ovalbumin to peptide-specific T cells was also compromised in a similar manner in *αGalA*$^{-/-}$ and *αGalA*$^{-/-}$/*iGb3S*$^{-/-}$ but not in *αGalA*$^{-/-}$/*Gb3S*$^{-/-}$ DCs (Fig. 7D). Together these results suggest that the storage of globosides leads to a functional alteration in the lysosomal compartment of DCs and subsequent impairment of antigen presentation.

Cholesterol overload induced by acetylated LDL similarly affected antigen presentation

It has been shown that GSL storage leads to intracellular cholesterol accumulation (57, 58). We hypothesized that cholesterol/cholesteryl ester overload might be one mechanism responsible for the disturbed antigen presentation in *αGalA*$^{-/-}$ (and also in *αGalA*$^{-/-}$/*iGb3S*$^{-/-}$) DCs. To test this, we induced cholesterol overload by exogenous administration of acetylated low-density lipoproteins (AcLDL) to WT bone marrow-derived DCs (BMDCs) and investigated their antigen presentation capacity. Cellular lipid accumulation could be documented by Oil Red O stain (Fig. S2A) and caused a significant decrease both in αGalCer presentation and in ovalbumin presentation and cross-presentation (Fig. S2B and C).

DISCUSSION

iGb3 has been proposed to be the endogenous ligand essential for thymic iNKT cell development (31). Although expression of iGb3S mRNA has been repeatedly documented in murine tissues including thymus (51, 59), the presence of iGb3 in murine thymus has remained controversial. This is based mainly on the fact that iGb3 and Gb3 are isomers differing solely in the glycosidic linkage of the terminal galactose moiety (Fig. 1), which makes a sensitive discrimination between iGb3 and the much more abundant Gb3 technically extremely challenging. Using a highly sensitive HPLC assay, which allowed detection of iGb3 when present at above 1% of the Gb3 level, iGb3 could not be detected in murine thymus in WT mice (34). In contrast, analyzing murine thymi by electrospray ionization-linear ion trap-mass spectrometry (ESI-LIT-MS^n) Li et al. were able to document signals that could be attributed to iGb3 in an iGb3/Gb3 ratio of 0.4% (33).

To solve this discrepancy, we have generated a *Gb3S*$^{-/-}$ mouse (Fig. 2) enabling us to address the presence of iGb3 in the absence of its isomer Gb3. To further increase the amounts of the putatively present iGb3, we crossed *Gb3S*$^{-/-}$ mice with *αGalA*$^{-/-}$ mice (murine model of Fabry disease, unable to degrade Gb3 and iGb3, resulting in their supra-physiological levels, Fig. 1). This approach allowed us to detect approximately 1600 molecules of iGb3 per thymocyte in *αGalA*$^{-/-}$/*Gb3S*$^{-/-}$ mice (Fig. 3) demonstrating that iGb3 can be synthesized in murine thymus although it does not indicate whether iGb3 is present under physiological conditions in this organ. This is because this genotype represents an extreme situation, as *Gb3S* deletion causes an increase of LacCer (Fig. 2D), which is also the substrate for iGb3S, and furthermore, once synthesized, iGb3 cannot be degraded due to *αGalA*-deficiency in these mice. In agreement with this, iGb3 has previously not been reported to be detectable in WT thymus using the same method (34) and was also not detectable in *Gb3S*$^{-/-}$ mice, i.e. in the absence of storage (Fig. 3). Moreover

these findings also lead to the conclusion that *iGb3S* is the only enzyme responsible for iGb3 synthesis as its trace quantities detected in $\alpha GalA^{-/-}/Gb3S^{-/-}$ mice were absent in $\alpha GalA^{-/-}/Gb3S^{-/-}/iGb3S^{-/-}$ triple knockout thymocytes, making the existence of an alternative pathway for iGb3 synthesis in mice very unlikely.

The amount of approximately 1600 molecules of iGb3 per thymocyte in $\alpha GalA^{-/-}/Gb3S^{-/-}$ mice (and presumably even lower in WT) seems to be low in terms of structural biology. Nevertheless it might still be enough to mediate a positive selection of iNKT cells as it has been shown that even a single antigen-MHC complex can elicit a response in conventional T cells (60, 61). Therefore we readdressed the question of whether depletion of these small iGb3 amounts in congenic iGb3-deficient mice would alter the iNKT cell population. However, backcrossing $iGb3S^{-/-}$ mice more than 10 times to the C57BL/6 genetic background still did not result in any alteration in iNKT cell numbers in $iGb3S^{-/-}$ as compared with WT mice. We hypothesized that the absence of iGb3 might still be reflected by alterations in the CDR3 region, which is a part of the interface between the invariant iNKT TCR and iGb3 loaded on CD1d molecules (62). However, the CDR3 region of iNKT cells was preserved despite the absence of iGb3 (Fig. 4), further strengthening the conclusion that iGb3 does not function as the decisive endogenous iNKT selecting ligand.

Brennan et al. have recently shown that GlcCer itself (in particular containing the N-acyl chain $C_{24:1}$) is recognized by iNKT cells, and that recognition of GlcCer-loaded CD1d-molecules is responsible for activation of iNKT cells by DCs upon recognition of microbial danger signals (41). It still remains to be elucidated whether GlcCer also plays a role as the endogenous lipid ligand in the process of thymic iNKT cell selection. However, considering GlcCer as the endogenous ligand for iNKT cell selection might be one explanation for the paradox that iNKT cell development remains unaffected by deficiency of particular GSL groups downstream of GlcCer in the biosynthetic pathway (Fig. 1). The *in vivo* proof of such a hypothesis would be technically very challenging as mice deficient in glucosylceramide synthase (GCS, the enzyme responsible for GlcCer synthesis, Fig. 1) die early during embryogenesis and working with a conditional knockout or GCS-inhibitor is associated with residual traces of GlcCer (63, 64). An alternative explanation has been provided by Facciotti et al., who have shown that peroxisome-derived ether-bonded mono-alkyl glycerophosphates are important for iNKT cell development (35).

Interestingly, until now alterations of the iNKT cell population have been documented only in mouse models in which the degradation but not the synthesis of GSLs was blocked. The mechanistic basis for this has been controversial. Based on the finding that iGb3 stimulated iNKT cells *in vitro*, Zhou et al. attributed the decreased iNKT cell numbers in $Hexb^{-/-}$ mice to decreased lysosomal iGb3 levels as these mice cannot degrade iGb4 to iGb3 (31) (Fig. 1). However, a decrease in the iNKT cell population has been documented in multiple other mouse models of lysosomal GSL storage disease (including $\alpha GalA^{-/-}$ mice) irrespective of the specific genetic defect or lipid stored (65, 66). Darmoise et al. have suggested that in $\alpha GalA^{-/-}$ mice the linking mechanism might be an overstimulation and increased apoptosis of iNKT cells due to iGb3 accumulation, although the accumulation or presence of iGb3 has not been addressed directly (40). If iGb3-storage would indeed mediate the iNKT cell phenotype in $\alpha GalA^{-/-}$ mice, then in $\alpha GalA^{-/-}/iGb3S^{-/-}$ mice the alterations would be predicted to return to normal. Contrary to this hypothesis, we demonstrate that iNKT cell numbers are decreased to the same extent in $\alpha GalA^{-/-}$ and $\alpha GalA^{-/-}/iGb3S^{-/-}$ mice (Fig. 5) thus implicating strongly that iGb3 cannot be the explanation for the diminished iNKT cell numbers in $\alpha GalA^{-/-}$ mice. Moreover, we have found a significant general reduction in the antigen presenting capacity of $\alpha GalA^{-/-}$ and $\alpha GalA^{-/-}/iGb3S^{-/-}$ splenic DCs (Fig. 7) and reason, in line with a previous publication (65), that all these phenomena are a consequence of storage *per se*. To prove this, we have performed ultrastructural and biochemical analysis

of spleens and documented an accumulation and derangement of lysosomal morphology in both *αGalA*$^{-/-}$ and *αGalA*$^{-/-}$/*iGb3S*$^{-/-}$ mice (Fig. 6). On TLC the pattern of accumulated GSL remained identical in *αGalA*$^{-/-}$ and *αGalA*$^{-/-}$/*iGb3S*$^{-/-}$ mice, with the major contributor to the storage being Gb3 (Fig. 6). Thus, in order to provide conclusive evidence that storage - and not the accumulation of iGb3 - is the real reason for all the morphological and physiological derangements in the function of *αGalA*$^{-/-}$ DCs, we have crossed these mice with *Gb3S*$^{-/-}$ and demonstrated that *αGalA*$^{-/-}$/*Gb3S*$^{-/-}$ mice, which are devoid of storage (Fig. 6), do not show any functional disturbance in antigen presentation or thymic selection of iNKT cells (Figs. 5 and 7). In this context it is interesting to note that recently Macedo et al. reported that α-galactosidase A enzyme replacement corrected the iNKT cell deficiency in *αGalA*$^{-/-}$ mice, however this approach does not allow to discriminate between the effects of the storage of globosides and isoglobosides (67).

Previous studies have shown that cellular GSL storage may promote cholesterol accumulation (58, 68). Supporting evidence has been published by Glaros et al. demonstrating that apolipoprotein A-I-mediated cholesterol efflux was inhibited in fibroblasts treated with lactosylceramide or a specific glucocerebrosidase inhibitor as well as in fibroblasts from patients with genetic GSL storage diseases (including *αGalA*-deficiency) (57). First indications that cholesterol metabolism may influence iNKT homeostasis were provided by Gadola et al., who showed decreased iNKT cell numbers and a defect in αGalCer presentation in the murine model for Niemann-Pick disease type C1 (NPC1) (65). Keeping in mind that NPC1 mice store not only cholesterol but also GSL, we tested whether the storage of cholesterol itself can impede antigen presentation and could show that in WT BMDCs cholesterol overload by AcLDL could hinder the presentation of peptide and lipid antigens (Fig. S2) similarly to the phenotype seen in *αGalA*$^{-/-}$ and *αGalA*$^{-/-}$/*iGb3S*$^{-/-}$ mice (Fig. 7). This is congruent with several other findings that imply that hypercholesterolemia and the presence of modified lipoproteins adversely affect the function of antigen presenting cells (69-71) although no difference in ovalbumin presentation between unloaded and AcLDL-loaded BMDCs was observed by Packard et al. (72). Based on our results we suggest that the cholesterol accumulation that accompanies GSL storage diseases may be one mechanism responsible for the described malfunctioning antigen presentation in *αGalA*$^{-/-}$ and *αGalA*$^{-/-}$/*iGb3S*$^{-/-}$ mice.

Upon exposure to heat-killed *E. coli,* DCs from *αGalA*$^{-/-}$ and *αGalA*$^{-/-}$/*iGb3S*$^{-/-}$ mice showed a reduced stimulatory capacity towards iNKT cells in comparison to WT DCs. In contrast, in *αGalA*$^{-/-}$/*Gb3S*$^{-/-}$ DCs the iNKT cell stimulation remained undistinguishable from WT (Fig. 7C). Notably there was no difference between WT and iGb3-deficient DCs in their iNKT cell stimulatory capacity upon exposure to heat-killed *E. coli* (Fig. 7C). This is in line with our previous results demonstrating that iGb3-deficient myeloid-derived suppressor cells (MDSC) can activate iNKT cells after TLR stimulation (73). Also injection of iGb3, even at a tenfold higher dose than αGalCer, did not elicit measurable IFNγ and IL-4 levels *in vivo* (data not shown).

Altogether, these results indicate that iGb3, despite its presence in the thymus and its ability to weakly activate iNKT cells *in vitro*, is unlikely to play a major role *in vivo* during positive selection of iNKT cells in the thymus or to modulate TLR-mediated crosstalk between DCs and iNKT cells in the periphery. Instead, using a direct genetic approach these results demonstrate that as a consequence of lipid storage, the interaction of DCs and iNKT cells is disturbed irrespective of iGb3-accumulation or lack thereof and provide further evidence that this interaction is not mediated by iGb3.

Europe PMC Funders Author Manuscripts

Supplementary Material

Refer to Web version on PubMed Central for supplementary material.

Acknowledgments

We thank F. van der Hoeven and U. Kloz for blastocyst microinjection; S. Kaden for excellent technical assistance (all at the German Cancer Research Center, Heidelberg, Germany), the NIH Tetramer Core Facility at Emory University, Atlanta, USA for providing PBS57-loaded CD1d tetramers, A. Kulkarni for providing α-galactosidase A-deficient mice (at the National Institutes of Health, Bethesda, MD, USA) and R. L. Proia (at the National Institutes of Health, Bethesda, MD, USA) for providing mice deficient for GalNAc-transferase, GM3-synthase and GD3-synthase.

REFERENCES

1. Makino Y, Kanno R, Ito T, Higashino K, Taniguchi M. Predominant expression of invariant V alpha 14+ TCR alpha chain in NK1.1+ T cell populations. Int Immunol. 1995; 7:1157–1161. [PubMed: 8527413]
2. Arase H, Arase N, Ogasawara K, Good RA, Onoe K. An NK1.1+ CD4+8-single-positive thymocyte subpopulation that expresses a highly skewed T-cell antigen receptor V beta family. Proc Natl Acad Sci U S A. 1992; 89:6506–6510. [PubMed: 1378629]
3. Kronenberg M, Gapin L. The unconventional lifestyle of NKT cells. Nat Rev Immunol. 2002; 2:557–568. [PubMed: 12154375]
4. Lantz O, Bendelac A. An invariant T cell receptor alpha chain is used by a unique subset of major histocompatibility complex class I-specific CD4+ and CD4-8-T cells in mice and humans. J Exp Med. 1994; 180:1097–1106. [PubMed: 7520467]
5. Lee PT, Benlagha K, Teyton L, Bendelac A. Distinct functional lineages of human V(alpha)24 natural killer T cells. J Exp Med. 2002; 195:637–641. [PubMed: 11877486]
6. Brigl M, Brenner MB. CD1: antigen presentation and T cell function. Annu Rev Immunol. 2004; 22:817–890. [PubMed: 15032598]
7. Hansen DS, Schofield L. Regulation of immunity and pathogenesis in infectious diseases by CD1d-restricted NKT cells. Int J Parasitol. 2004; 34:15–25. [PubMed: 14711586]
8. Taniguchi M, Harada M, Kojo S, Nakayama T, Wakao H. The regulatory role of Valpha14 NKT cells in innate and acquired immune response. Annu Rev Immunol. 2003; 21:483–513. [PubMed: 12543936]
9. Van Kaer L, Parekh VV, Wu L. Invariant natural killer T cells: bridging innate and adaptive immunity. Cell Tissue Res. 2011; 343:43–55. [PubMed: 20734065]
10. Shimoda S, Tsuneyama K, Kikuchi K, Harada K, Nakanuma Y, Nakamura M, Ishibashi H, Hisamoto S, Niiro H, Leung PS, Ansari AA, Gershwin ME, Akashi K. The role of natural killer (NK) and NK T cells in the loss of tolerance in murine primary biliary cirrhosis. Clin Exp Immunol. 2012; 168:279–284. [PubMed: 22519590]
11. Das R, Sant'Angelo DB, Nichols KE. Transcriptional control of invariant NKT cell development. Immunol Rev. 2010; 238:195–215. [PubMed: 20969594]
12. Salio M, Silk JD, Cerundolo V. Recent advances in processing and presentation of CD1 bound lipid antigens. Curr Opin Immunol. 2010; 22:81–88. [PubMed: 20080041]
13. Kinjo Y, Ueno K. iNKT cells in microbial immunity: recognition of microbial glycolipids. Microbiol Immunol. 2011; 55:472–482. [PubMed: 21434991]
14. Kronenberg M, Kinjo Y. Innate-like recognition of microbes by invariant natural killer T cells. Curr Opin Immunol. 2009; 21:391–396. [PubMed: 19646850]
15. Kawano T, Cui J, Koezuka Y, Toura I, Kaneko Y, Motoki K, Ueno H, Nakagawa R, Sato H, Kondo E, Koseki H, Taniguchi M. CD1d-restricted and TCR-mediated activation of valpha14 NKT cells by glycosylceramides. Science. 1997; 278:1626–1629. [PubMed: 9374463]
16. Morita M, Motoki K, Akimoto K, Natori T, Sakai T, Sawa E, Yamaji K, Koezuka Y, Kobayashi E, Fukushima H. Structure-activity relationship of alpha-galactosylceramides against B16-bearing mice. J Med Chem. 1995; 38:2176–2187. [PubMed: 7783149]

17. Wei DG, Curran SA, Savage PB, Teyton L, Bendelac A. Mechanisms imposing the Vbeta bias of Valpha14 natural killer T cells and consequences for microbial glycolipid recognition. J Exp Med. 2006; 203:1197–1207. [PubMed: 16651387]
18. Chiu YH, Park SH, Benlagha K, Forestier C, Jayawardena-Wolf J, Savage PB, Teyton L, Bendelac A. Multiple defects in antigen presentation and T cell development by mice expressing cytoplasmic tail-truncated CD1d. Nat Immunol. 2002; 3:55–60. [PubMed: 11731798]
19. Smiley ST, Kaplan MH, Grusby MJ. Immunoglobulin E production in the absence of interleukin-4-secreting CD1-dependent cells. Science. 1997; 275:977–979. [PubMed: 9020080]
20. Honey K, Benlagha K, Beers C, Forbush K, Teyton L, Kleijmeer MJ, Rudensky AY, Bendelac A. Thymocyte expression of cathepsin L is essential for NKT cell development. Nat Immunol. 2002; 3:1069–1074. [PubMed: 12368909]
21. Zhou D, Cantu C 3rd, Sagiv Y, Schrantz N, Kulkarni AB, Qi X, Mahuran DJ, Morales CR, Grabowski GA, Benlagha K, Savage P, Bendelac A, Teyton L. Editing of CD1d-bound lipid antigens by endosomal lipid transfer proteins. Science. 2004; 303:523–527. [PubMed: 14684827]
22. Gapin L. iNKT cell autoreactivity: what is 'self' and how is it recognized? Nat Rev Immunol. 2010; 10:272–277. [PubMed: 20224567]
23. Porcelli SA, Modlin RL. The CD1 system: antigen-presenting molecules for T cell recognition of lipids and glycolipids. Annu Rev Immunol. 1999; 17:297–329. [PubMed: 10358761]
24. Cox D, Fox L, Tian R, Bardet W, Skaley M, Mojsilovic D, Gumperz J, Hildebrand W. Determination of cellular lipids bound to human CD1d molecules. PLoS One. 2009; 4:e5325. [PubMed: 19415116]
25. Muindi K, Cernadas M, Watts GF, Royle L, Neville DC, Dwek RA, Besra GS, Rudd PM, Butters TD, Brenner MB. Activation state and intracellular trafficking contribute to the repertoire of endogenous glycosphingolipids presented by CD1d [corrected]. Proc Natl Acad Sci U S A. 2010; 107:3052–3057. [PubMed: 20133624]
26. Yuan W, Kang SJ, Evans JE, Cresswell P. Natural lipid ligands associated with human CD1d targeted to different subcellular compartments. J Immunol. 2009; 182:4784–4791. [PubMed: 19342656]
27. Pei B, Speak AO, Shepherd D, Butters T, Cerundolo V, Platt FM, Kronenberg M. Diverse endogenous antigens for mouse NKT cells: self-antigens that are not glycosphingolipids. J Immunol. 2011; 186:1348–1360. [PubMed: 21191069]
28. Gumperz JE, Roy C, Makowska A, Lum D, Sugita M, Podrebarac T, Koezuka Y, Porcelli SA, Cardell S, Brenner MB, Behar SM. Murine CD1d-restricted T cell recognition of cellular lipids. Immunity. 2000; 12:211–221. [PubMed: 10714687]
29. Stanic AK, De Silva AD, Park JJ, Sriram V, Ichikawa S, Hirabyashi Y, Hayakawa K, Van Kaer L, Brutkiewicz RR, Joyce S. Defective presentation of the CD1d1-restricted natural Va14Ja18 NKT lymphocyte antigen caused by beta-D-glucosylceramide synthase deficiency. Proc Natl Acad Sci U S A. 2003; 100:1849–1854. [PubMed: 12576547]
30. Xia C, Yao Q, Schumann J, Rossy E, Chen W, Zhu L, Zhang W, De Libero G, Wang PG. Synthesis and biological evaluation of alpha-galactosylceramide (KRN7000) and isoglobotrihexosylceramide (iGb3). Bioorg Med Chem Lett. 2006; 16:2195–2199. [PubMed: 16458002]
31. Zhou D, Mattner J, Cantu C 3rd, Schrantz N, Yin N, Gao Y, Sagiv Y, Hudspeth K, Wu YP, Yamashita T, Teneberg S, Wang D, Proia RL, Levery SB, Savage PB, Teyton L, Bendelac A. Lysosomal glycosphingolipid recognition by NKT cells. Science. 2004; 306:1786–1789. [PubMed: 15539565]
32. Porubsky S, Speak AO, Luckow B, Cerundolo V, Platt FM, Grone HJ. Normal development and function of invariant natural killer T cells in mice with isoglobotrihexosylceramide (iGb3) deficiency. Proc Natl Acad Sci U S A. 2007; 104:5977–5982. [PubMed: 17372206]
33. Li Y, Thapa P, Hawke D, Kondo Y, Furukawa K, Hsu FF, Adlercreutz D, Weadge J, Palcic MM, Wang PG, Levery SB, Zhou D. Immunologic glycosphingolipidomics and NKT cell development in mouse thymus. J Proteome Res. 2009; 8:2740–2751. [PubMed: 19284783]
34. Speak AO, Salio M, Neville DC, Fontaine J, Priestman DA, Platt N, Heare T, Butters TD, Dwek RA, Trottein F, Exley MA, Cerundolo V, Platt FM. Implications for invariant natural killer T cell

ligands due to the restricted presence of isoglobotrihexosylceramide in mammals. Proc Natl Acad Sci U S A. 2007; 104:5971–5976. [PubMed: 17372214]

35. Facciotti F, Ramanjaneyulu GS, Lepore M, Sansano S, Cavallari M, Kistowska M, Forss-Petter S, Ni G, Colone A, Singhal A, Berger J, Xia C, Mori L, De Libero G. Peroxisome-derived lipids are self antigens that stimulate invariant natural killer T cells in the thymus. Nat Immunol. 2012; 13:474–480. [PubMed: 22426352]
36. Brigl M, Brenner MB. How invariant natural killer T cells respond to infection by recognizing microbial or endogenous lipid antigens. Semin Immunol. 2010; 22:79–86. [PubMed: 19948416]
37. Paget C, Mallevaey T, Speak AO, Torres D, Fontaine J, Sheehan KC, Capron M, Ryffel B, Faveeuw C, Leite de Moraes M, Platt F, Trottein F. Activation of invariant NKT cells by toll-like receptor 9-stimulated dendritic cells requires type I interferon and charged glycosphingolipids. Immunity. 2007; 27:597–609. [PubMed: 17950005]
38. Salio M, Speak AO, Shepherd D, Polzella P, Illarionov PA, Veerapen N, Besra GS, Platt FM, Cerundolo V. Modulation of human natural killer T cell ligands on TLR-mediated antigen-presenting cell activation. Proc Natl Acad Sci U S A. 2007; 104:20490–20495. [PubMed: 18077358]
39. Mattner J, Debord KL, Ismail N, Goff RD, Cantu C 3rd, Zhou D, Saint-Mezard P, Wang V, Gao Y, Yin N, Hoebe K, Schneewind O, Walker D, Beutler B, Teyton L, Savage PB, Bendelac A. Exogenous and endogenous glycolipid antigens activate NKT cells during microbial infections. Nature. 2005; 434:525–529. [PubMed: 15791258]
40. Darmoise A, Teneberg S, Bouzonville L, Brady RO, Beck M, Kaufmann SH, Winau F. Lysosomal alpha-galactosidase controls the generation of self lipid antigens for natural killer T cells. Immunity. 2010; 33:216–228. [PubMed: 20727792]
41. Brennan PJ, Tatituri RV, Brigl M, Kim EY, Tuli A, Sanderson JP, Gadola SD, Hsu FF, Besra GS, Brenner MB. Invariant natural killer T cells recognize lipid self antigen induced by microbial danger signals. Nat Immunol. 2011; 12:1202–1211. [PubMed: 22037601]
42. Muyrers JP, Zhang Y, Stewart AF. Techniques: Recombinogenic engineering--new options for cloning and manipulating DNA. Trends Biochem Sci. 2001; 26:325–331. [PubMed: 11343926]
43. Schwenk F, Baron U, Rajewsky K. A cre-transgenic mouse strain for the ubiquitous deletion of loxP-flanked gene segments including deletion in germ cells. Nucleic Acids Res. 1995; 23:5080–5081. [PubMed: 8559668]
44. Sango K, Johnson ON, Kozak CA, Proia RL. beta-1,4-N-Acetylgalactosaminyltransferase involved in ganglioside synthesis: cDNA sequence, expression, and chromosome mapping of the mouse gene. Genomics. 1995; 27:362–365. [PubMed: 7558008]
45. Yamashita T, Hashiramoto A, Haluzik M, Mizukami H, Beck S, Norton A, Kono M, Tsuji S, Daniotti JL, Werth N, Sandhoff R, Sandhoff K, Proia RL. Enhanced insulin sensitivity in mice lacking ganglioside GM3. Proc Natl Acad Sci U S A. 2003; 100:3445–3449. [PubMed: 12629211]
46. Kawai H, Allende ML, Wada R, Kono M, Sango K, Deng C, Miyakawa T, Crawley JN, Werth N, Bierfreund U, Sandhoff K, Proia RL. Mice expressing only monosialoganglioside GM3 exhibit lethal audiogenic seizures. J Biol Chem. 2001; 276:6885–6888. [PubMed: 11133999]
47. Ohshima T, Murray GJ, Swaim WD, Longenecker G, Quirk JM, Cardarelli CO, Sugimoto Y, Pastan I, Gottesman MM, Brady RO, Kulkarni AB. alpha-Galactosidase A deficient mice: a model of Fabry disease. Proc Natl Acad Sci U S A. 1997; 94:2540–2544. [PubMed: 9122231]
48. Lehuen A, Lantz O, Beaudoin L, Laloux V, Carnaud C, Bendelac A, Bach JF, Monteiro RC. Overexpression of natural killer T cells protects Valpha14-Jalpha281 transgenic nonobese diabetic mice against diabetes. J Exp Med. 1998; 188:1831–1839. [PubMed: 9815260]
49. Exley MA, Bigley NJ, Cheng O, Shaulov A, Tahir SM, Carter QL, Garcia J, Wang C, Patten K, Stills HF, Alt FW, Snapper SB, Balk SP. Innate immune response to encephalomyocarditis virus infection mediated by CD1d. Immunology. 2003; 110:519–526. [PubMed: 14632651]
50. Adachi O, Kawai T, Takeda K, Matsumoto M, Tsutsui H, Sakagami M, Nakanishi K, Akira S. Targeted disruption of the MyD88 gene results in loss of IL-1- and IL-18-mediated function. Immunity. 1998; 9:143–150. [PubMed: 9697844]

51. Porubsky S, Wang S, Kiss E, Dehmel S, Bonrouhi M, Dorn T, Luckow B, Brakebusch C, Grone HJ. Rhoh deficiency reduces peripheral T-cell function and attenuates allogenic transplant rejection. Eur J Immunol. 2011; 41:76–88. [PubMed: 21182079]
52. Malle E, Ibovnik A, Stienmetz A, Kostner GM, Sattler W. Identification of glycoprotein IIb as the lipoprotein(a)-binding protein on platelets. Lipoprotein(a) binding is independent of an arginyl-glycyl-aspartate tripeptide located in apolipoprotein(a). Arterioscler Thromb. 1994; 14:345–352. [PubMed: 8123637]
53. Malle E, Hazell L, Stocker R, Sattler W, Esterbauer H, Waeg G. Immunologic detection and measurement of hypochlorite-modified LDL with specific monoclonal antibodies. Arterioscler Thromb Vasc Biol. 1995; 15:982–989. [PubMed: 7541296]
54. Chomczynski P, Sacchi N. Single-step method of RNA isolation by acid guanidinium thiocyanate-phenol-chloroform extraction. Anal Biochem. 1987; 162:156–159. [PubMed: 2440339]
55. Pannetier C, Cochet M, Darche S, Casrouge A, Zoller M, Kourilsky P. The sizes of the CDR3 hypervariable regions of the murine T-cell receptor beta chains vary as a function of the recombined germ-line segments. Proc Natl Acad Sci U S A. 1993; 90:4319–4323. [PubMed: 8483950]
56. Betz J, Bielaszewska M, Thies A, Humpf HU, Dreisewerd K, Karch H, Kim KS, Friedrich AW, Muthing J. Shiga toxin glycosphingolipid receptors in microvascular and macrovascular endothelial cells: differential association with membrane lipid raft microdomains. J Lipid Res. 2011; 52:618–634. [PubMed: 21252262]
57. Glaros EN, Kim WS, Quinn CM, Wong J, Gelissen I, Jessup W, Garner B. Glycosphingolipid accumulation inhibits cholesterol efflux via the ABCA1/apolipoprotein A-I pathway: 1-phenyl-2-decanoylamino-3-morpholino-1-propanol is a novel cholesterol efflux accelerator. J Biol Chem. 2005; 280:24515–24523. [PubMed: 15890646]
58. Puri V, Watanabe R, Dominguez M, Sun X, Wheatley CL, Marks DL, Pagano RE. Cholesterol modulates membrane traffic along the endocytic pathway in sphingolipid-storage diseases. Nat Cell Biol. 1999; 1:386–388. [PubMed: 10559968]
59. Milland J, Christiansen D, Lazarus BD, Taylor SG, Xing PX, Sandrin MS. The molecular basis for galalpha(1,3)gal expression in animals with a deletion of the alpha1,3galactosyltransferase gene. J Immunol. 2006; 176:2448–2454. [PubMed: 16456004]
60. Stone JD, Chervin AS, Kranz DM. T-cell receptor binding affinities and kinetics: impact on T-cell activity and specificity. Immunology. 2009; 126:165–176. [PubMed: 19125887]
61. Sykulev Y, Joo M, Vturina I, Tsomides TJ, Eisen HN. Evidence that a single peptide-MHC complex on a target cell can elicit a cytolytic T cell response. Immunity. 1996; 4:565–571. [PubMed: 8673703]
62. Zajonc DM, Savage PB, Bendelac A, Wilson IA, Teyton L. Crystal structures of mouse CD1d-iGb3 complex and its cognate Valpha14 T cell receptor suggest a model for dual recognition of foreign and self glycolipids. J Mol Biol. 2008; 377:1104–1116. [PubMed: 18295796]
63. Jennemann R, Sandhoff R, Wang S, Kiss E, Gretz N, Zuliani C, Martin-Villalba A, Jager R, Schorle H, Kenzelmann M, Bonrouhi M, Wiegandt H, Grone HJ. Cell-specific deletion of glucosylceramide synthase in brain leads to severe neural defects after birth. Proc Natl Acad Sci U S A. 2005; 102:12459–12464. [PubMed: 16109770]
64. Yamashita T, Wada R, Sasaki T, Deng C, Bierfreund U, Sandhoff K, Proia RL. A vital role for glycosphingolipid synthesis during development and differentiation. Proc Natl Acad Sci U S A. 1999; 96:9142–9147. [PubMed: 10430909]
65. Gadola SD, Silk JD, Jeans A, Illarionov PA, Salio M, Besra GS, Dwek R, Butters TD, Platt FM, Cerundolo V. Impaired selection of invariant natural killer T cells in diverse mouse models of glycosphingolipid lysosomal storage diseases. J Exp Med. 2006; 203:2293–2303. [PubMed: 16982810]
66. Sagiv Y, Hudspeth K, Mattner J, Schrantz N, Stern RK, Zhou D, Savage PB, Teyton L, Bendelac A. Cutting edge: impaired glycosphingolipid trafficking and NKT cell development in mice lacking Niemann-Pick type C1 protein. J Immunol. 2006; 177:26–30. [PubMed: 16785493]

67. Macedo MF, Quinta R, Pereira CS, Sa Miranda MC. Enzyme replacement therapy partially prevents invariant Natural Killer T cell deficiency in the Fabry disease mouse model. Mol Genet Metab. 2012

68. Puri V, Jefferson JR, Singh RD, Wheatley CL, Marks DL, Pagano RE. Sphingolipid storage induces accumulation of intracellular cholesterol by stimulating SREBP-1 cleavage. J Biol Chem. 2003; 278:20961–20970. [PubMed: 12657626]

69. de Bont N, Netea MG, Demacker PN, Verschueren I, Kullberg BJ, van Dijk KW, van der Meer JW, Stalenhoef AF. Apolipoprotein E knock-out mice are highly susceptible to endotoxemia and Klebsiella pneumoniae infection. J Lipid Res. 1999; 40:680–685. [PubMed: 10191292]

70. Ludewig B, Jaggi M, Dumrese T, Brduscha-Riem K, Odermatt B, Hengartner H, Zinkernagel RM. Hypercholesterolemia exacerbates virus-induced immunopathologic liver disease via suppression of antiviral cytotoxic T cell responses. J Immunol. 2001; 166:3369–3376. [PubMed: 11207293]

71. Shamshiev AT, Ampenberger F, Ernst B, Rohrer L, Marsland BJ, Kopf M. Dyslipidemia inhibits Toll-like receptor-induced activation of CD8alpha-negative dendritic cells and protective Th1 type immunity. J Exp Med. 2007; 204:441–452. [PubMed: 17296788]

72. Packard RR, Maganto-Garcia E, Gotsman I, Tabas I, Libby P, Lichtman AH. CD11c(+) dendritic cells maintain antigen processing, presentation capabilities, and CD4(+) T-cell priming efficacy under hypercholesterolemic conditions associated with atherosclerosis. Circ Res. 2008; 103:965–973. [PubMed: 18832748]

73. De Santo C, Salio M, Masri SH, Lee LY, Dong T, Speak AO, Porubsky S, Booth S, Veerapen N, Besra GS, Grone HJ, Platt FM, Zambon M, Cerundolo V. Invariant NKT cells reduce the immunosuppressive activity of influenza A virus-induced myeloid-derived suppressor cells in mice and humans. J Clin Invest. 2008; 118:4036–4048. [PubMed: 19033672]

74. Muthing J, Schweppe CH, Karch H, Friedrich AW. Shiga toxins, glycosphingolipid diversity, and endothelial cell injury. Thromb Haemost. 2009; 101:252–264. [PubMed: 19190807]

Europe PMC Funders Author Manuscripts

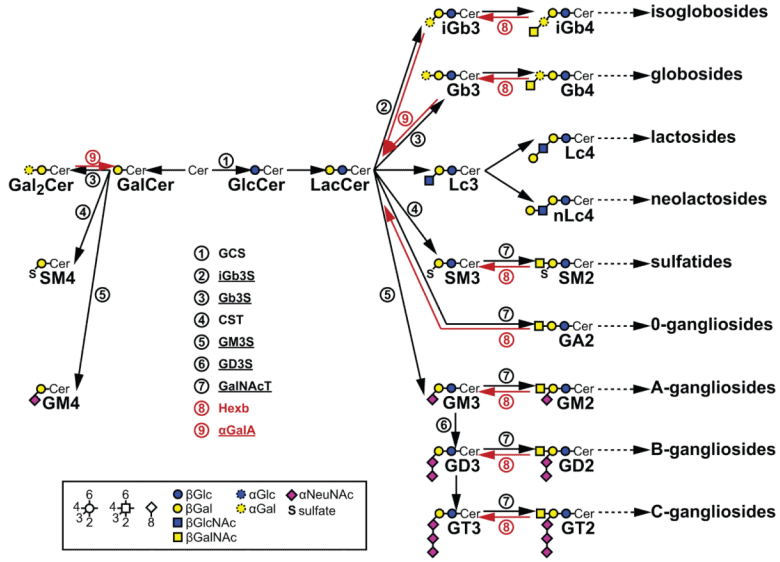

Figure 1. Metabolic GSL pathways

Shown are the most prominent mammalian groups of GSL with the two principal branches of GSL, which are based either on glactosyl ceramide (GalCer) or glucosyl ceramide (GlcCer). GlcCer is invariably processed to lactosyl ceramide (LacCer). By subsequent action of further enzymes on either GalCer or LacCer individual groups of GSL emerge, of which the most important are displayed. Relevant synthesis (black) and degradation (red) enzymes are indicated as encircled numbers: 1, GlcCer synthase (GCS); 2, isoglobotrihexosylceramide (iGb3) synthase (iGb3S); 3, globotrihexosylceramide (Gb3) synthase (Gb3S); 4, cerebroside sulfotransferase (CST); 5, GM3 synthase (GM3S); 6, GD3 synthase (GD3S); 7, GalNAc transferase (GalNAcT); 8, β-hexosaminidase (Hexb) and 9, α-galactosidase A (αGalA). Enzymes investigated in this study are underlined.

Europe PMC Funders Author Manuscripts

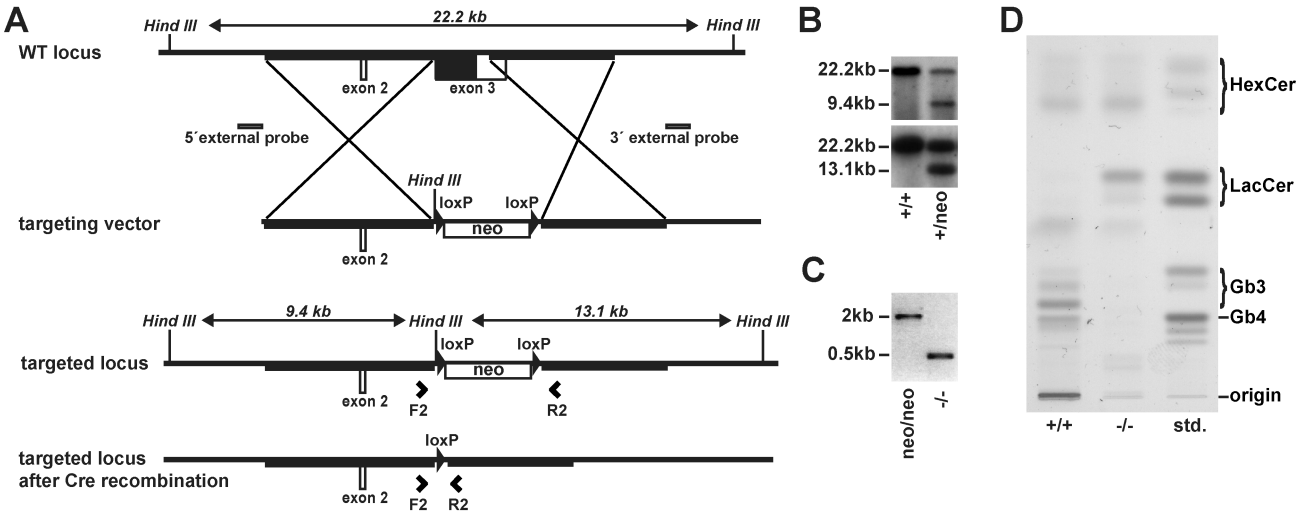

Figure 2. Generation of Gb3 synthase-deficient mice

A: Targeting strategy showing murine *Gb3S* wild type (WT) locus, targeting vector and the targeted locus before and after Cre-mediated recombination together with HindIII restriction sites and probes for Southern blot analysis. Coding and non-coding regions of exons 2 and 3 are depicted as filled and open boxes, respectively. Homology arms are shown as bold lines. Arrowheads show the position and orientation of PCR primers. Triangles flanking the PGK-gb2-neomycin selection cassette (neo) symbolize loxP sequences.

B: Southern blot analysis of the genomic DNA from embryonic stem cells using 5′ and 3′ external probes, as indicated in (A) showed shortening of the diagnostic 22.2kb long HindIII fragment present in WT (+/+) down to 9.4 and 13.1kb respectively after homologous recombination (+/neo).

C: Cre-mediated deletion of the neomycin selection cassette was confirmed by PCR using forward (F2) and reverse (R2) primers as a shortening of the 2048bp-long product to 498bp. neo/neo and −/− represent homozygous animals with targeted loci before and after Cre-mediated deletion of the neomycin selection cassette.

D: TLC analysis of neutral GSL isolated from kidneys of wild type (+/+) and *Gb3S*-deficient (−/−) mice showed absence of Gb3 and its downstream products such as Gb4. As a consequence, the precursor substance lactosylceramide (LacCer) was increased. As standard (std.) an extract of neutral GSL from human spleen was used. Orcinol stain. HexCer, hexosylceramide.

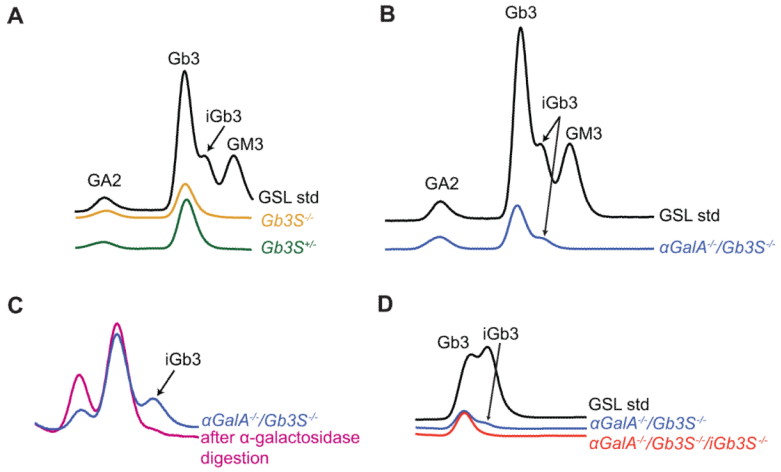

Figure 3. HPLC analysis of thymi demonstrated the presence of minute amounts of iGb3 in *αGalA*$^{-/-}$/*Gb3S*$^{-/-}$ mice

Single cell suspensions were prepared from murine thymi. After determining the cell number, homogenates were processed for HPLC.

A: In both heterozygous controls and *Gb3S*$^{-/-}$ mice iGb3 was undetectable in thymus.

B: The presence of iGb3 could be documented in thymi of *αGalA*$^{-/-}$/*Gb3S*$^{-/-}$ mice, which accumulated only isoglobosides but no globosides.

C: The iGb3 peak was fully susceptible to α-galactosidase digestion. In contrast, the peak co-migrating with Gb3 was unsusceptible to α-galactosidase digestion.

D: The iGb3 peak was absent in *αGalA*$^{-/-}$/*Gb3S*$^{-/-}$/*iGb3S*$^{-/-}$ triple knockout mice.

Europe PMC Funders Author Manuscripts

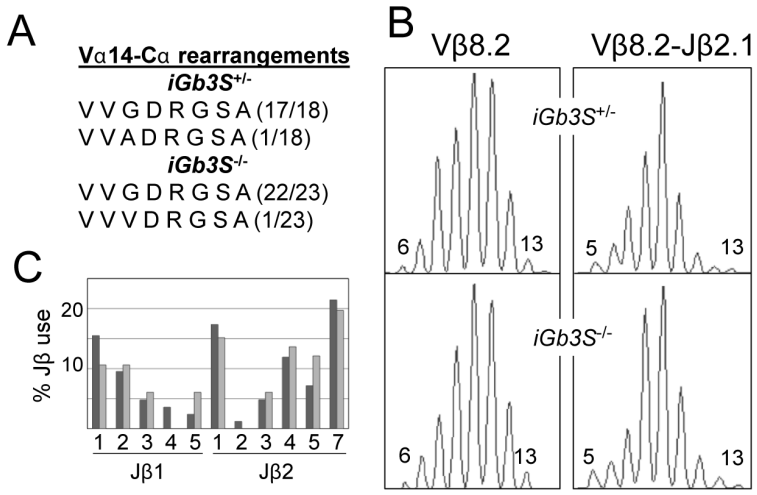

Figure 4. iGb3S$^{-/-}$ mice expressed a typical iNKT TCR repertoire

iNKT thymocytes from *iGb3S*$^{-/-}$ and control (*iGb3S*$^{+/-}$) mice were analyzed for TCR usage.

A: The canonical iNKT Vα14-Jα18 CDR3 sequence was dominant in *iGb3S*$^{-/-}$ and control mice.

B: Total Vβ8.2 (left plots) and Vβ8.2-Jβ2.1 (right plots) TCRs in *iGb3S*$^{-/-}$ (lower plots) and control mice (upper plots) had highly similar CDR3 size distribution spectratypes. CDR3 lengths are indicated.

C: Proportional Jβ segment use within Vβ8.2 CDR3 regions of iNKT cells was conserved in the absence of iGb3. Darker and lighter columns are iGb3-deficient and control samples respectively. Only functional Jβ gene segments are shown.

Europe PMC Funders Author Manuscripts

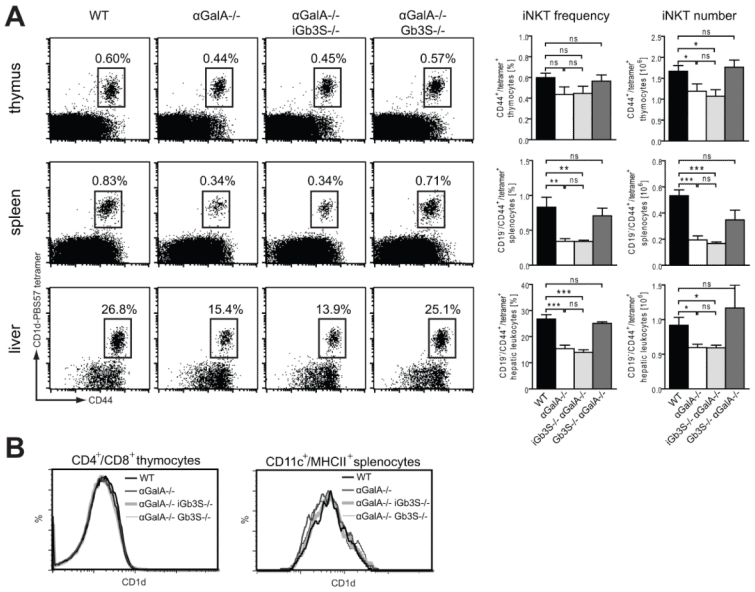

Figure 5. iNKT cell phenotype of *αGalA*$^{-/-}$ storage mice could be reverted by the absence of globosides but not by the absence of isoglobosides

A: Frequencies and absolute numbers of iNKT cells were measured by flow cytometry in 26 week old WT, *αGalA*$^{-/-}$, *αGalA*$^{-/-}$/*iGb3S*$^{-/-}$ and *αGalA*$^{-/-}$/*Gb3S*$^{-/-}$ mice using PBS57-loaded CD1d-tetramers and anti-CD44 antibodies. In case of spleen and liver CD19^{+} cells were gated out. In *αGalA*$^{-/-}$ storage mice the iNKT cell population showed a significant reduction in spleens and livers in both relative and absolute numbers; in thymi the reduction was statistically significant only for absolute iNKT cell numbers. In *αGalA*$^{-/-}$ /*iGb3S*$^{-/-}$ mice the additional *iGb3S* deficiency did not influence this phenotype. In contrast, in *αGalA*$^{-/-}$/*Gb3S*$^{-/-}$ mice the absence of globosides restored iNKT cell numbers to WT levels. Bars represent means ± SEM; n=6-8/group; *, p<0.05; **, p<0.01; ***, p<0.001; ns, not significant.

B: Neither of the genotypes influenced CD1d expression on double positive (CD4^{+}/CD8^{+}) thymocytes and splenic DCs (CD11c^{+}/MHCII^{+}) as analyzed by flow cytometry.

Europe PMC Funders Author Manuscripts

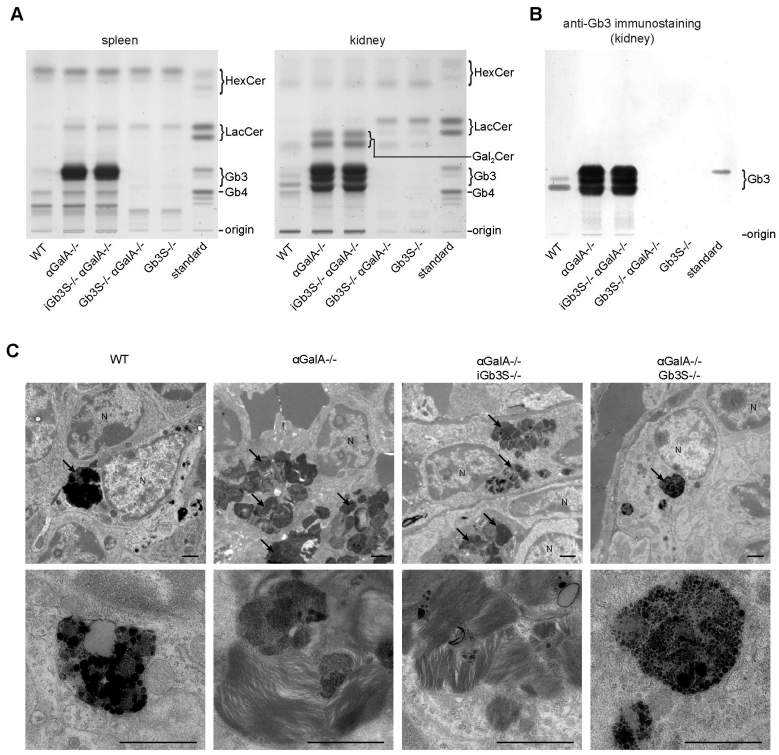

Figure 6. Globosides were the major GSL stored in *αGalA*$^{-/-}$ splenocytes leading to a severe lysosomal derangement

A: TLC-analysis of neutral GSL from spleens and kidneys of WT, *αGalA*$^{-/-}$, *αGalA*$^{-/-}$ / *iGb3S*$^{-/-}$, *αGalA*$^{-/-}$/*Gb3S*$^{-/-}$ and *Gb3S*$^{-/-}$ mice. In spleens and kidneys of *αGalA*$^{-/-}$ storage mice the major accumulating GSL run at the height of Gb3. Additional deficiency for iGb3S did not affect the composition of neutral GSL in *αGalA*$^{-/-}$/*iGb3S*$^{-/-}$ mice. In contrast, in *αGalA*$^{-/-}$/*Gb3S*$^{-/-}$ mice the accumulation of globosides (and galabiosylceramide, Gal_2Cer, in kidney) was absent. An extract of neutral GSL from human spleen was used as a standard and orcinol staining was performed for visualization. Heterogeneity in the composition of fatty acid moieties results in some GSL (e.g. Gb3) running as multiple bands (74).

B: A TLC plate with renal neutral GSL, which was run in parallel with the one shown in (A) was immnostained with polyclonal Gb3-specific antibody JM06/298-1 (56), which identified the majority of the GSL stored in *αGalA*$^{-/-}$ and *αGalA*$^{-/-}$/*iGb3S* mice to be Gb3.

C: Splenic white pulp of 26-week old mice was analyzed by transmission electron microscopy. WT splenocytes showed a regular morphology of lysosomes (arrows). In contrast, splenocytes of *αGalA*$^{-/-}$ mice were characterized by severely distorted lysosomal architecture with multiple enlarged lysosomes containing abundant lamellar inclusions. This was the case also when isoglobosides were depleted in *αGalA*$^{-/-}$/*iGb3S*$^{-/-}$ mice. However, in *αGalA*$^{-/-}$/*Gb3S*$^{-/-}$ mice the depletion of globosides restored the lysosomal architecture to a state morphologically indistinguishable from WT. Scale bar corresponds to 1μm. N, nucleus.

Europe PMC Funders Author Manuscripts

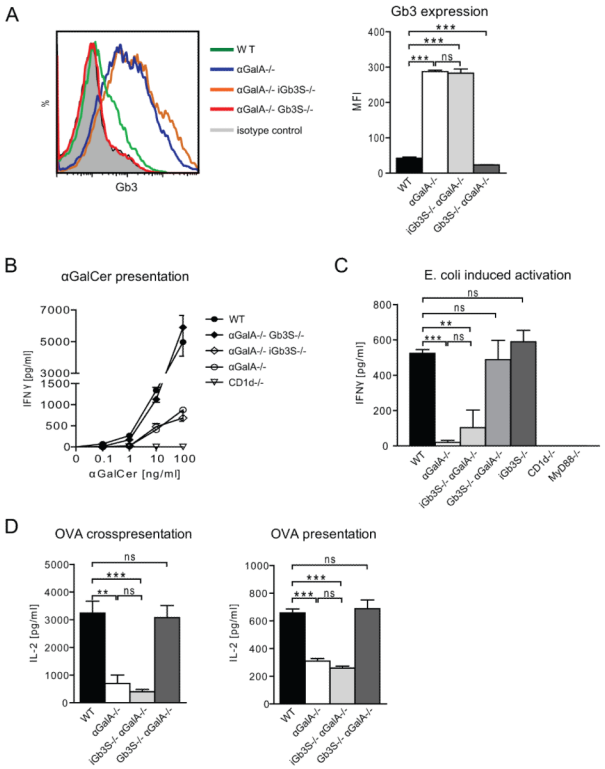

Figure 7. DCs from *αGalA*$^{-/-}$ mice showed a profound defect in antigen presentation including a weaker induction of antimicrobial response by iNKT cells

A: Splenic DCs (enriched by anti-CD11c magnetic beads), which were used for all further experiments, were stained with rat monoclonal IgM anti-Gb3 primary antibody (38-13) in combination with FITC-labeled anti-rat IgM secondary antibody. Flow cytometry demonstrated that Gb3 was expressed at low levels in WT, but accumulated extensively in *αGalA*$^{-/-}$ DCs. This accumulation was absent in *αGalA*$^{-/-}$/*Gb3S*$^{-/-}$ but not in *αGalA*$^{-/-}$/*iGb3S*$^{-/-}$ DCs. Bars represent means ± SEM; n=3/group.

B: In splenic DCs, antigen presentation by CD1d was assessed by exposure to different αGalCer concentrations followed by co-incubation with WT iNKT cells. Presentation of αGalCer on *αGalA*$^{-/-}$ DCs was significantly diminished throughout the whole range of concentrations tested. Similarly *αGalA*$^{-/-}$/*iGb3S*$^{-/-}$ DCs showed an impaired αGalCer presentation. This derangement could be returned to normal after depleting the stored globosides in *αGalA*$^{-/-}$/*Gb3S*$^{-/-}$ DCs. *CD1d*$^{-/-}$ DCs served as negative controls. Shown are means ± SEM; n=4/group.

C: DC-mediated microbial activation of iNKT cells was tested by applying heat-killed *E. coli* to DCs followed by co-incubation with WT iNKT cells. As for αGalCer, the activation capacity of *αGalA*$^{-/-}$ and *αGalA*$^{-/-}$/*iGb3S*$^{-/-}$ DCs was significantly lower in comparison to WT and only the abrogation of storage could restore normal function in *αGalA*$^{-/-}$/*Gb3S*$^{-/-}$ DCs. In *iGb3S* deficient DCs the microbe-elicited activation of iNKT cells was unaffected. *CD1d*$^{-/-}$ and *MyD88*$^{-/-}$ DCs served as negative controls. Bars represent means ± SEM; n=4/group.

D: The ability of splenic DCs to process and (cross)present ovalbumin (OVA) was investigated. To this end OVA-exposed DCs from the indicated phenotypes were allowed to interact with MHCII- or MHCI-restricted WT T-cell hybridomas and supernatant IL-2 was measured. Both antigen presentation and cross-presentation activity was significantly disturbed on *αGalA*$^{-/-}$ and *αGalA*$^{-/-}$/*iGb3S*$^{-/-}$ DCs in comparison to WT. DCs from *αGalA*$^{-/-}$/*Gb3S*$^{-/-}$ mice showed an unaltered antigen (cross)presentation activity.

Bars represent means ± SEM; n=3/group. **, p<0.01; ***, p<0.001; ns, not significant.

Europe PMC Funders Author Manuscripts